Porosity Study of Hybrid Silica Mesostructure in Aluminium Oxide Membrane Columnar by Cyclic Voltammetry Method

M.N. Jalil[a]*, H.M. Zaki[a], R.A.W. Dryfe[b] and M.W. Anderson[b]

[a]Faculty of Applied Sciences, Universiti Teknologi MARA, 40450 Shah Alam
Selangor Darul Ehsan, Malaysia
[b]Centre of Nanoporous Materials, School of Chemistry, The University of Manchester United Kingdom

*Corresponding email: moham423@salam.uitm.edu.my

Abstract

Silica mesostructure has been grown within with a porous aluminium oxide membrane columnar material (hybrid-AOM). This was prepared using a sol-gel technique with Pluronic P123 triblock copolymer as the structure-directing agent and tetraethyl orthosilicate as the inorganic source. The porosity of the hybrid-AOM after ethanol extraction was calculated from the cyclic voltammetry response of a neutral probe (FcMeOH), using Randles-Sevčik equation.

Keywords: Porosity Study, Hybrid Silica Mesostructure, Aluminium Oxide Membrane, Voltammetry Method

1.   INTRODUCTION

The synergetic coupling between sol-surfactant chemistry and inorganic membranes as hybrids has opened new avenues for advanced materials research. Indeed, the ability to position 'organized matter' at the nano-scale inside membrane pores such as commercial aluminium oxide membrane (AOM) has been a significant breakthrough [1,2].

Aluminium oxide in a form of membrane or powder is an inorganic compound with the chemical formula of Al_2O_3. Aluminium oxide offered a good chemical, thermal [3] and mechanical stability and not necessarily to be used as a filter [4] catalyst or filler. Aluminium oxide membrane (AOM) in particular, is normally made from anodizing a very thin aluminium sheet in acid electrolytes such as sulphuric acid. As a result, the aluminium oxide membrane which has relatively regular pore is produced [3]. AOM has been used as template or backbone for other materials such as nanowire [5-7] and growing silica mesostructure [1,8]. Apart from that, the free standing AOM with mesostructure within its columnar (hybrid-AOM) can be used in wide variety of fields such as separation, catalysis and adsorption. The hybrid-AOM pore size can be tailored by growing different type of mesostructure and this provides the applications opportunity for wide verity of molecular size.

Many researchers have tried to find the best technique to insert silica mesostructures into AOM and to characterise the resultant hybrid materials. [1,2,8-11]. To the best knowledge, none of the work mentioned in the literature really discusses about the packing of mesostructure inside the AOM columns and the redox species permeability through the free standing hybrid-AOM. Therefore, it is wise to address this question, because a good packing and ion permeability will reflect the truly porosity of hybrid-AOM and its mesostructural character. Hence the objective of this paper was to study the hybrid-AOM active surface area and porosity using voltammetry method (cyclic voltammetry, CV) using ferrocene methanol as a redox active probe.

2.   EXPERIMENTAL

Chemicals and reagents

AOM was purchased from Whatman with a thickness of 60 μm, pore diameter of ca. 0.2 μm and disc diameter of 13 mm. Pluronic P123, with an average molecular weight of 5800 g mol^{-1}, was purchased from Aldrich. TEOS (98 %) was used as the silica source for hybrid-AOM synthesis and was purchased from Aldrich. Ethanol and hydrochloric acid, of analytical grade, were purchased from Fisher Scientific. For electrochemical experiments, the ferrocene methanol (FcMeOH) and potassium potassium phthalate (KHP) buffer were purchased from sigma Aldrich. All solutions were prepared with high-purity water (18 MΩ cm) from a Millipore "milli-Q" water purification system.

Hybrid-aluminium oxide membrane (hybrid-AOM) synthesis

Synthesis of the hybrid-AOM template started with the preconditioning of the substrate. AOM was heated at 110 °C for 5 minutes prior to use to ensure that the membrane was free from moisture, which can cause blockages in the AOM pore channels. The hybrid-AOM precursor solution was prepared by mixing 10 g of P123, 50 ml of ethanol and 2 g of 1M hydrochloric acid. The mixture was stirred at 35 °C for 2 hours, then 20.08 g of TEOS were slowly added to the solution and the mixture was stirred for a further hour at the same temperature. The samples were left at room temperature (gelling process) with an open lid for 4 days and the gelled solution was then heated in the oven at 90 °C for 24 hours [2]. The samples obtained were then carefully separated from the dried gel using filter paper. The product was a free-standing membrane with silica structures inside its pores, which was named as hybrid-AOM. The hybrid-AOM was then

soaking with ethanol for 24 hours to leach out the surfactant template and make the material porous [12,13].

Electrochemical experiments
Electrochemical experiments were run in an electrochemical cell made in-house. Cyclic voltammograms were performed using an electrode setup where the membrane material was set as the working electrode with an open area of 0.123 cm^2 (0.4 cm diameter), platinum gauze as the counter electrode and Ag/AgCl as the reference electrode. A membrane electrode, Aluminium oxide membrane (AOM) and hybrid-aluminium oxide membrane (hybrid-AOM) were fabricated by evaporating high purity gold (99.9999 %) onto one side of our samples. Pure gold deposition rate was controlled at around 0.1-0.3 Å/s to the thickness of 1 μM.
The electrochemical solution comprised 500 μM FcMeOH in 500 mM KHP (pH 4). As a comparison, a commercial gold electrode of 0.031 cm^2 (0.2 cm diameter) was used as a working electrode. All electrochemical experiments were performed with a PGSTAT20 Autolab potentiostat controlled by the GPES electrochemical software (Eco Chemie).

Scanning electron microscopy (SEM) and X-ray diffraction (XRD) experiments
Scanning electron micrographs were taken using an FEI Quanta 200 Philips XL-30 with field emission gun (FEG). The samples were prepared by attaching them to double-sided carbon tape, then were mounted onto an aluminium microscope holder and sputtered with a thin layer of gold to reduce charging.
XRD patterns were collected from a Bruker AXS D8 Advance powder X-ray diffractometer using Cu Kα radiation (λ = 1.5418 Å). The powder samples were packed carefully into an aluminium holder and pressed with a glass slide to ensure a flat, smooth sample surface. Patterns were typically recorded from 2θ = 0.4^o to 6.0^o.

3. RESULTS AND DISCUSSION

Permeability of porous materials such as hybrid-AOM can be studied electrochemically, since the presence of pores of molecular dimensions allows redox probes to diffuse selectively through the materials to an underlying electrode surface to undergo redox processes. The large surface-to-volume ratios and the variations of geometry in hybrid-AOM should strongly affect the transport properties of redox species through this mesoporous material. The voltammetric responses, which deviate from those of a smooth electrode, are the electrochemical characteristics of a porous surface. Since electrochemistry is concerned with electrodes and currents, the preparation of electrodes on top from mesostructured materials is a major consideration in electrochemical studies [14]. Therefore one of mesostructure sides was covered with pure gold (~1 μm)
Ferrocene methanol was chosen as the redox active species because it is soluble in water and undergoes a simple one-electron reversible oxidation to the cation [15]. It was important to use a neutral redox species in order to eliminate the factor of surface charge, which might have upset the permeability of the solute through the pores. In the presence of potential the FcMeOH will undergo the following redox process:

$$\text{FcMeOH}_{(aq)} \rightleftharpoons \text{FcMeOH}^+_{(aq)} + e^- \tag{1}$$

Modification of the working electrode with AOM leads to various limiting cases arising for the currents observed. Under the experimental conditions, voltammetric techniques can be employed, since each ion transferring from the aqueous phase has to travel through a pore, leading to the various possible diffusion fields and assimilated determination of the porosity.
According to the Randles-Sevčik equation [16] for an ideal planar diffusion and reversible electrons transfer, the magnitude of the peak current, I_p, in the cyclic voltammogram is a function of the temperature (T), bulk concentration (C), electrode area, the number of electrons transferred (n), the diffusion coefficient (D) and scan rate (v). The equation is as follows:

$$I_p = 0.4463nFA\left(\frac{nF}{RT}\right)^{1/2} D^{1/2} v^{1/2} C \qquad (2)$$

In this equation, F is Faraday's constant (96485 C / mol), R is the universal gas constant (8.314 J / mol K) and T is the absolute temperature (K). It is noted that if the temperature is assumed to be 25 °C (298.15 K), the Randles-Sevčik equation can be written in a briefer form:

$$I_p = (2.687\text{x}10^5)\, n^{3/2} v^{1/2} D^{1/2} A\, C \qquad (3)$$

where v is the scan rate in Vs^{-1}, D is the diffusion coefficient in $cm^2 s^{-1}$, A is the area in cm^{-2} and C is the concentration in $molcm^{-3}$.

In case of a porous electrode made from non-conducting materials, the porous material has to be attached to a conductor. Thus, with a non-conductor on the surface of a conductor, the actual active area is much lower than the original area. Therefore, the Randles-Sevčik equation can be rewritten as follows [17]:

$$I_p = (2.687x10^5)n^{3/2}v^{1/2}D^{1/2}\varphi AC \qquad (4)$$

Here, φ is known as the porosity; for porous media such as AOM and hybrid-AOM, it can be defined as the fraction of void area (active electrode area) on the electrode compared to the original electrode area, as in the following equation. Assuming that other parameters are constant and only the active area is reduced by the presence of porous materials on top of the electrode, hence (5) is significant.

$$\varphi = \frac{A_v}{A_t} = \frac{I_v}{I_t} \qquad (5)$$

where A_v is the active area of the electrode, A_t is the total bulk electrode area (commercial gold film), φ is a fraction between 0 and 1, I_v is the current obtained from the modified porous electrode (AOM gold film or hybrid-AOM) and I_t is the current obtained from the commercial gold electrode.
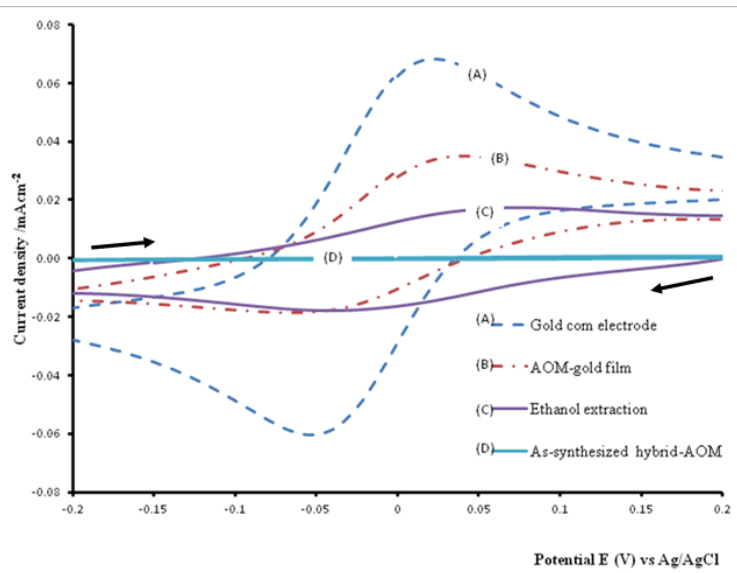

Figure 1: Cyclic voltammograms for (A) gold commercial electrode, (B) As purchased aluminium oxide membrane, (C) porous hybrid-aluminium oxide membrane (hybrid-AOM after ethanol extraction for 24 hours) and (D) as-synthesized hybrid-AOM. All samples except gold commercial electrode were covered with gold film on one of its side. The Cyclic voltammograms are recorded in 0.05 M potassium phthalate buffer solution (pH 4) containing 500 μM FcMeOH at 0.05 V/s scan rate.

As shown in Figure 1, before surfactant extraction, the magnitude of the faradaic current was very low (Figure 1 (D)). The CV response in this case is typical for a physical barrier limiting probe diffusion through hybrid-AOM from the solution to the evaporated electrode surface [18]. However, dissolved ions such as Cl$^-$ in the surfactant template gave some conductivity to the as-synthesized hybrid-AOM film. Therefore, by comparing the background current observed for as-synthesized hybrid-AOM (2×10^{-3} mAcm^{-2}) with the redox current for bare gold electrode (12.84×10^{-2} mAcm^{-2}, (Figure 1 (B)), it is estimated that without surfactant removal, the sample blocked 98.4 % of the current from reaching the underlying electrode.

Moreover, CVs for Empty-AOM (Figure 1 (B)) and a commercial gold electrode (Figure 1 (A)) can be compares. Empty-AOM shows a low current density as compared to the commercial electrode. Since I_p is proportional to the electrode area, A, the porosity (φ) can be estimated using (5). The current density of the AOM-gold film (2.17×10^{-5} Acm^{-2}) is divided by the gold commercial electrode (7.03×10^{-5} Acm^{-2}), giving a value of φ for the Empty-AOM of 0.31. This means that about one-third of the whole AOM membrane is composed of pores and the rest is the AOM wall. The ratio thus explains the porosity of the blank AOM (Empty-AOM). This result is within the range of porosity values claimed by the manufacturers (25 to 50 %) [4]. It also agrees with Platt *et al*. ($\varphi = 0.3$) [19] where a similar AOM membrane was used but probed using liquid/liquid voltammetry. The actual active area of the AOM-gold film electrode is then calculated to be $A_v = 0.04 \ cm^2$

The estimated active area of the Empty-AOM electrode was 0.04 cm^2, compared to the original area (electrode without AOM) of 0.13 cm^2. This shows that the active area has been reduced by the presence of a structured material on the electrode surface so that only part of the electrode was exposed to the electrolyte, while the rest was covered by alumina.

The electrochemical experiments and electrode preparation for hybrid-AOM were the same as for the Empty-AOM. Basically, gold film was evaporated onto one side of a hybrid-AOM sample which had first been soaked in ethanol for 24 hours. The membrane with gold film coating was then used as a working electrode. When hybrid-AOM was used as the working electrode, the redox peaks shape and position were similar to the AOM-gold film but differ in term of the background current (larger) with lower current density. These data prove that the AOM pores had been filled with porous structure which then covered some of electrode area and consequently reduced the active area. The estimated porosity was based on (5) and the ratio of current between hybrid-AOM (ethanol extraction sample, 6.97×10^{-6} Acm^{-2}) and gold commercial electrode (7.03×10^{-5} Acm^{-2}), giving a φ value of 0.1.

The φ of hybrid-AOM quoted here was forecast comes from a combination of the diffusion of redox species through the mesostructure and the gap between the AOM columns and the actual mesostructure. This argument is supported by the SEM cross-sectional image of hybrid-AOM in Figure 2 (D), which shows that the mesostructure has filled the AOM columns but with some defects and cracks between mesostructure columns. The XRD analysis (Figure 3) also shows that there was shrinking evident of the macrostructure after surfactant removal via ethanol extraction as illustrated in Figure 3.
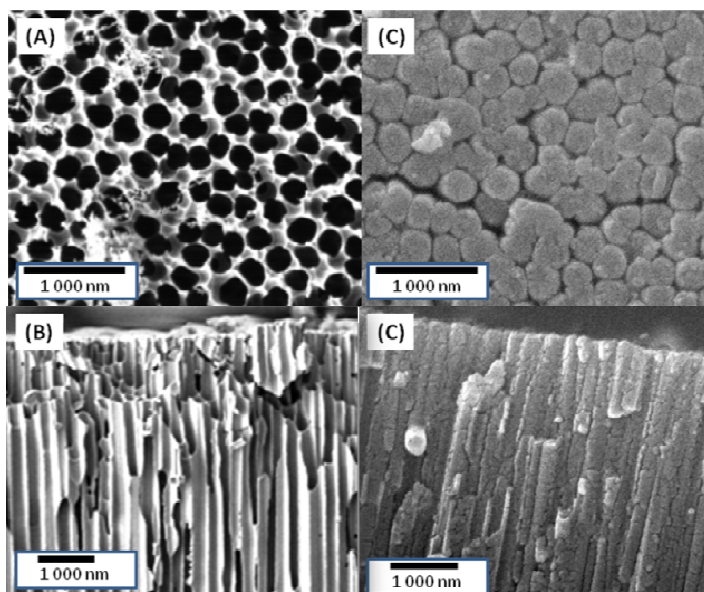
Figure 2: Field emission scanning electron microscopy (FE-SEM) images of A) top view B) cross sectional view of as-purchased aluminium oxide membrane (AOM). Images of C) top view and D) cross sectional view of hybrid-aluminium oxide membrane (hybrid-AOM) after ethanol extraction for 24 hours.

The SEM morphology of the as-purchased AOM is shown in Figure 2 (A). From the SEM images, it was estimated that the mean pore diameter was between 200 and 300 nm. Thus, the AOM can be categorized as a macroporous structure [20]. All pores were facing towards the SEM detector but differed slightly in size and shape: Figure 2 (C) shows the orientations of the pore channels were parallel to each other. The SEM image in Figure 2 (B) is the hybrid-AOM after soaking with ethanol. It shows that, the mesoporous material seems to have swollen rather than shrunk, so that it fills the AOM pores completely and protrudes above the surface level; indeed, in the cross-sectional view (image D) it is difficult to differentiate between the AOM pore walls and the mesostructure.

The hybrid-AOM sample was further characterized using powder SAXRD (Figure 3) to confirm the structural stability of the mesostructure material after surfactant removal. All sample shows only one diffraction peak with low angle XRD [21], it is suggested that these materials can be identified as an amorphous material with mesostructured characteristics. The shift in peak position for as-synthesized sample to a higher 2θ value after surfactant removal (ethanol and calcination) indicates that there was significant reduction in the respective d-spacing values. The number of diffraction peak remains the same before and after surfactant removal. This indicates the preservation of the hybrid-AOM structure upon template removal by ethanol or thermal extraction (calcination).
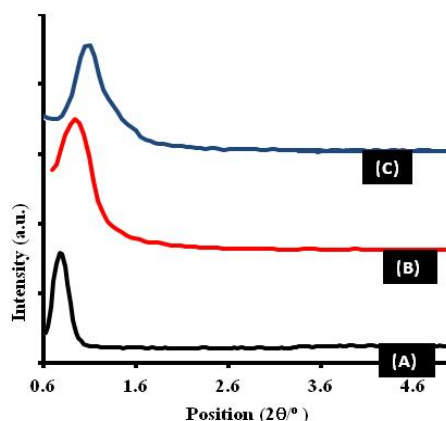
Figure 3: Small-angle X-ray diffraction patterns (SAXRD) of hybrid-aluminium oxide membrane (hybrid-AOM) for A) as-synthesized sample, B) ethanol extraction for 24 hours and C) calcined at 500 °C (1°/min) for 4 hours in air.

4.   CONCLUSIONS

The electrochemical study of mesostrusture porosity revealed that the AOM-gold film had a porosity of 0.31, whilst with mesostructure growth in the AOM columns; the porosity of hybrid-AOM was reduced to 0.1. The porosity of hybrid-AOM indicates the existence of interconnections pore within mesostructure after surfactant removal. Without surfactant removal, hybrid-AOM barred more than 98.4 % of current from reaching the underlying gold electrode, which indicates that before surfactant extraction, the mesostructure inside the AOM columns was fully packed.

REFERENCES

[1]   Sakamoto, Y.; Nagata, K.; Yogo, K.; Yamada, K. *Microporous and Mesoporous Materials* **2007**, *101*, 303-311.
[2]   Lu, Q.; Gao, F.; Komarneni, S.; Mallouk, T. *J. Am. Chem. Soc.* **2004**, *126*, 8650-8651.
[3]   Itaya, K.; Sugawara, S.; Arai, K.; Saito, S. *Journal of Chemical Engineering of Japan* **1984**, *17*, 514-520.
[4]   Whatman; Whatman plc: 2010; Vol. 2010-, p Communication from manufacturer.
[5]   Pang, Y. T.; Meng, G. W.; Zhang, L. D.; Shan, W. J.; Zhang, C.; Gao, X. Y.; Zhao, A. W.; Mao, Y. Q. *J. Solid State Electrochem.* **2003**, *7*, 344-347.
[6]   Preston, C. K.; Moskovits, M. *J. Phys. Chem.* **1993**, *97*, 8495-8503.
[7]   Routkevitch, D.; Bigioni, T.; Moskovits, M.; Xu, J. M. *J. Phys. Chem.* **1996**, *100*, 14037-14047.
[8]   Kumar, P.; Ida, J.; Kim, S.; Guliants, V. V.; Lin, J. Y. S. *Journal of Membrane Science* **2006**, *279*, 539-547.
[9]   Platschek, B.; Kohn, R.; Doblinger, M.; Bein, T. *Langmuir* **2008**, *24*, 5018-5023.
[10]   Platschek, B.; Köhn, R.; Döblinger, M.; Bein, T. *ChemPhysChem* **2008**, *9*, 2059-2067.
[11]   Platschek, B.; Petkov, N.; Bein, T. *Angew. Chem. Int. Ed.* **2006**, *45*, 1134-1138.
[12]   Joël, P. *Angew. Chem. Int. Ed.* **2004**, *43*, 3878-3880.
[13]   Ng, J. B. S.; Vasiliev, P. O.; Bergstro¨m, L. *Microporous and Mesoporous Materials* **2008**, *112*, 589-596.
[14]   Rusling, J. F.; Suib, S. L. *Adv. Mater.* **1994**, *6*, 922-930.
[15]   Etienne, M.; Quach, A.; Grosso, D.; Nicole, L.; Sanchez, C.; Walcarius, A. *Chem. Mater.* **2007**, *19*, 844-856.
[16]   Monk, P. M. S. *Fundamentals of electroanalytical chemistry*; John Wiley: Chichester, 2001.
[17]   Platt, M.; Dryfe, R. A. W.; Roberts, E. P. L. *Electrochimica Acta* **2003**, *48*, 3037-3046.
[18]   Sayen, S.; Walcarius, A. *Electrochemistry Communications* **2003**, *5*, 341-348.
[19]   Platt, M.; Dryfe, R. A. W.; Roberts, E. P. L. *Langmuir* **2003**, *19*, 8019-8025.
[20]   Sing, K. S. W.; Rouquerolt, J.; Avnir, D.; Fairbridge, C. W.; Everett, D. H.; Haynes, J. H.; Pernicone, N.; Ramsay, J. D. F.; Unger, K. K. *Pure & Appl. Chern* **1994**, *66*, 1739-1758.
[21]   Langford, J. I.; Louer, D. *Rep. Prog. Phys.* **1996**, *59*, 131-234.